Department of Medicine[1], City College, Wuhan University of Science and Technology; Faculty of Pharmacy[2], Hubei University of Chinese Medicine, Wuhan; Department of Blood Transfusion[3], Weifang People's Hospital, Weifang; Department of Pharmacy[4], Wuhan Fourth Hospital, Wuhan Puai Hospital, Tongji Medical College, Huazhong University of Science and Technology, Wuhan, China

Swertiamarin protects neuronal cells from oxygen glucose deprivation/reoxygenation via TLR4/PARP1/NF-κB pathway

Ji Wu[1,#], Fangfang Yang[2,#], Xinju Li[3], Tao Wu[4,*], Li Liu[4,*], Hongping Song[2,4,*]

Received January 30, 2019, accepted March 2, 2019

**Corresponding authors: Mrs. Hongping Song, Fangfang Yan, Tao Wu, Department of Pharmacy, Wuhan Fourth Hospital; Wuhan Puai Hospital, Tongji Medical College, Huazhong University of Science and Technology, Wuhan, China*
goodgravity@foxmail.com
[#]Theses authors contributed equally to this work.

Pharmazie: 481-484 74 (2019) *doi: 10.1691/ph.2019.9369*

Swertiamarin (STM) is a natural compound from *Swertia mussotii* Franch. (Gentianaceae) that exhibits various pharmacological effects. The current study tested the potential neuroprotective activity of STM in human neuroblastoma SH-SY5Y cells challenged with oxygen-glucose deprivation/reoxygenation (OGDR). Cell Counting Kit-8 assays were used to assess cell viability and the JC-1 assay were performed to evaluate changes in mitochondrial membrane potential (ΔΨm). The intracellular levels of ROS production were measured by 20,70-dichlorofuorescein diacetate (DCFH-DA) staining and flow cytometry. In addition, neuronal apoptosis was evaluated by staining with annexin V and flow cytometry. The determinations had also been made on TLR4-related proteins by Western blot analysis. Results show that exposure to OGDR significantly decreased cell viability but this decrease was attenuated by pretreatment with STM. STM also significantly attenuated declines in ΔΨm, inhibited OGDR-induced increases in intracellular ROS production, and reduced cell apoptosis. OGDR notably induced TLR4, Myd88, NF-κB p65 and PARP1 expression levels in the cells. However, treatment with STM reduced the expression of TLR4, Myd88, NF-κB p65 and PARP1. In conclusion, STM protected SH-SY5Y cells against OGDR-induced injury by attenuating increases in ROS levels and suppressing apoptosis, at least in part, via TLR4/PARP1/NF-κB pathway.

1. Introduction

Cerebral ischemia leads to significant human morbidities and mortalities (Fuentes and Tejedor 2014). It results in the deficiency of oxygen and nutrient supplies to the brain followed by neuronal injury (Yu et al. 2009). Reperfusion as the main treatment has achieved limited clinical success because of the secondary brain injury, which is referred to as ischemia and reperfusion injury (Molina and Alvarez-Sabín 2007). In cultured neuronal cell lines, oxygen-glucose deprivation and reoxygenation (OGDR) was applied to mimic the ischemia-reperfusion injuries *in vitro* (Park et al. 2017). OGDR-induced neuronal injury is a complicated process with complex mechanisms involving neuroinflammation, oxidative stress, mitochondrial dysfunction and apoptosis, which eventually lead to irreversible neuronal cell death and brain injury (Sun et al. 2016).

Inflammation is one of the most important factors causing brain damage after stroke (Macrez et al. 2011). Nuclear factor kappa B (NF-κB) is a major transcriptional regulator of neuroinflammation (del Zoppo 2010). The NF-κB p65/p50 heterodimer complexes with its inhibitory factor IκBα under a normal state and becomes inactive in the cytoplasm. The IκB kinase beta is rapidly phosphorylated after cerebral ischemia–reperfusion injury to induce IκBα phosphorylation and degradation. Then the p65/p50 dimer is released and transported to the nucleus, where it promotes the expression of pro-inflammatory genes (Kumar et al. 2011). A number of experiments showed that neuroprotectants notably inhibited the NF-κB pathway, suggesting that NF-κB contributed to ischemic brain injury (Mahesh et al. 2011; Zhang et al. 2014). The upstream regulators of NF-κB are toll-like receptors (TLRs), which play a vital role in neuronal apoptosis and injury (Ulbrich et al. 2015). Activation of TLR4 triggers the downstream stimulation of NF-κB inducing kinase and the pathway leading to activation of IkB kinases, which in turn phosphorylate IkB and promote its degradation (Régnier et al. 1997).

Swertiamarin (STM), an iridoid compound isolated from *Swertia mussotii* Franch (Gentianaceae) which is traditionally used as a traditional medicine in Tibet, China, exerts significant antioxidant and antiapoptosis effect in hepatic injury (Wu et al. 2017; Zhang et al. 2019). STM has been proved to protect the H_2O_2-induced cardiomyocytes apoptosis due to its antioxidant activity (Xu et al. 2010). We previously revealed that STM could inhibit TLR4 activation in experimental fibrosis (Wu et al. 2018). In this study, we aimed to explore the potential neuroprotective effects of STM on OGDR-induced neuronal injury.

2. Investigations and results

2.1. STM protects human neuronal cells against OGDR-stimulated cytotoxicity

CCK-8 assays were applied to inspect cytotoxicity of 30, 60 and 120 μM of STM on SH-SY5Y cells after 24 h incubation. The results show that there was no statistical significance in cell viability between the untreated control group and the 30, 60 and 120 μM STM treated groups, implying that the concentration of STM (30, 60 and 120 μM) chosen in present study was not cytotoxic (Fig. 1A).

Cell viability was detected using CCK-8 assays. As shown in Fig. 1B, a significant decrease in cell viability of the OGD/R group was observed compared with the control group ($p < 0.01$). Pretreatment with STM (30, 60 and 120 μM) significantly increased the cell viability compared with the OGD/R group ($p < 0.01$).

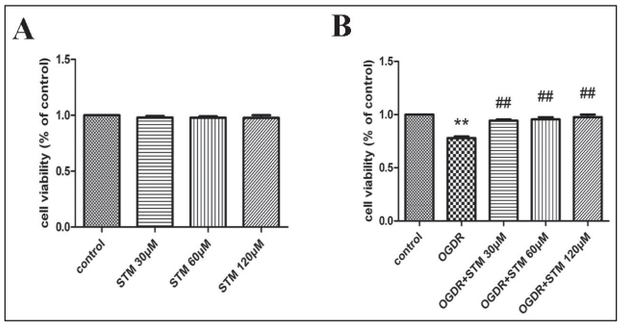

Fig. 1: STM protects human neuronal cells against OGDR-stimulated cytotoxicity. A: CCK-8 assays showed that there was no statistical significance in cell viability between untreated control group and STM (30, 60 and 120 μM) treated group. B: There was a significant decrease in the cell viability of the OGD/R group as compared with the control group ($p < 0.01$). Pretreatment with STM (30, 60 and 120 μM) increased the viability of SH-SY5Y cells subjected to OGD/R, with oxygen-glucose deprivation for 4 h and reoxygenation for 24 h ($p < 0.01$). All data were obtained from at least three independent experiments. The results are represented as means ± S.D. * $p < 0.05$ versus control, ** $p < 0.01$ versus control; $^{\#}$ $p < 0.05$ versus OGDR, $^{\#\#}$ $p < 0.01$ versus OGDR by one- way ANOVA and LSD post hoc test.

2.2. Attenuation of OGDR-induced mitochondrial dysfunction and elevation of ROS production by STM

A JC-1 assay was conducted to determine ΔΨm the of the SH-SY5Y cells. OGDR resulted in mitochondrial depolarization, which in turn may influence apoptotic processes in SH-SY5Y cells. OGDR reduced ΔΨm of the SH-SY5Y cells, pretreatment with STM resulted in an obvious increase in ΔΨm (Fig. 2A).

In this study, the cells were pretreated with STM for an hour and the levels of ROS were quantified using DCF-DA staining. OGDR significantly increased the intracellular levels of ROS in SH-SY5Y cells. And pretreatment with STM ((30, 60 and 120 μM)) reduced ROS production (Fig. 2B).

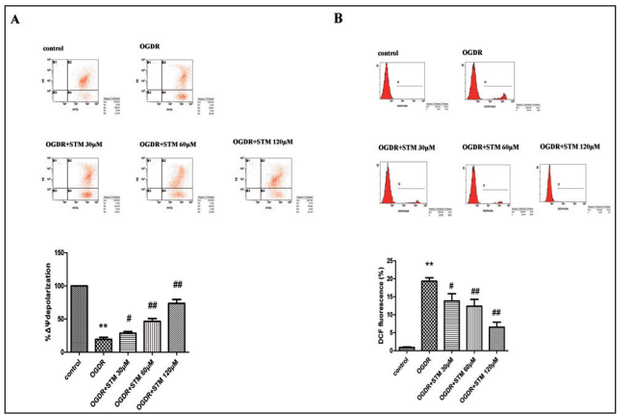

Fig. 2: Attenuation of OGDR-induced mitochondrial dysfunction and elevation of ROS production by STM. A: OGDR reduced ΔΨm of the SH-SY5Y cells, pretreatment with STM (30, 60 and 120 μM) resulted in an obvious increase in ΔΨm. B: OGDR significantly increased the intracellular levels of ROS in SH-SY5Y cells. Pretreatment with STM (30, 60 and 120 μM) reduced ROS production. All data were obtained from at least three independent experiments. The results are represented as means ± S.D. * $p < 0.05$ versus control, ** $p < 0.01$ versus control; $^{\#}$ $p < 0.05$ versus OGDR, $^{\#\#}$ $p < 0.01$ versus OGDR by one- way ANOVA and LSD post hoc test.

2.3. STM prevents OGDR-induced apoptosis of human neuronal cells

As shown in Fig. 3, apoptotic rates in the OGD/R group were was significantly higher than in the control group ($p < 0.01$). Pretreatment with STM (30, 60 and 120 μM) significantly decreased the apoptotic rate compared with OGD/R treatment alone ($p < 0.05$ or 0.01).

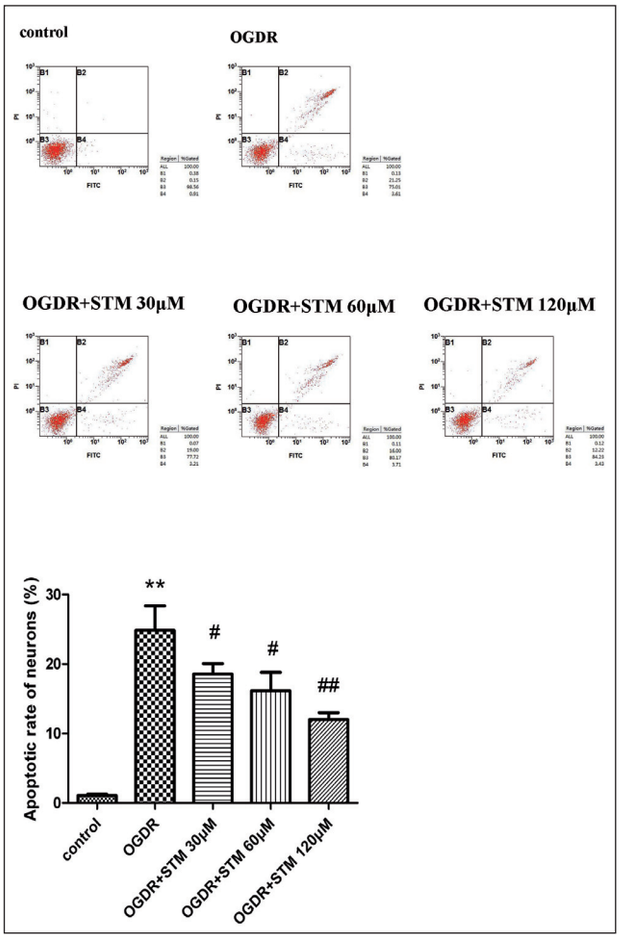

Fig. 3: STM prevents OGDR-induced apoptosis of human neuronal cells. The proportion of apoptotic cells was measured using an Annexin V-FITC/PI assay. The apoptotic rate was significantly higher in the OGD/R group than in the control group ($p < 0.01$). Pretreatment with STM (30, 60 and 120μM) significantly decreased the apoptotic rate compared with OGD/R treatment alone ($p < 0.05$ or 0.01). All data were obtained from at least three independent experiments. The results are represented as means ± S.D. * $p < 0.05$ versus control, ** $p < 0.01$ versus control; $^{\#}$ $p < 0.05$ versus OGDR, $^{\#\#}$ $p < 0.01$ versus OGDR by one- way ANOVA and LSD post hoc test.

2.4. STM inhibits the TLR4/PARP1/NF-κB signaling pathway

As shown in Fig. 4, the expression of TLR4, Myd88, PARP1 and NF-κB P65 protein in the OGD/R group was notably increased compared with the control group ($p < 0.01$). The expression of TLR4, Myd88, PARP1 and NF-κB P65 protein in the OGD/R group was notably increased compared with the control group ($p < 0.01$). In comparison, pretreatment with STM (30, 60 and 120 μM) significantly inhibited Myd88 and NF-κB P65 protein expression as compared with the OGD/R group ($p < 0.01$). Pretreatment with STM (60 and 120 μM) significantly reduced TLR4 protein expression as compared with the OGD/R group ($p < 0.01$). Pretreatment with STM (120 μM) significantly repressed PARP1 expression as compared with the OGD/R group ($p < 0.01$).

3. Discussion

In the present study, STM, an active compound of the traditional Chinese herb *Swertia mussotii* Franch (Gentianaceae), exhibited an inhibitory effect on TLR4 and the corresponding downstream PARP1 and NF-κB, subsequently relieved apoptosis, reduced ROS production in OGDR-stimulated human neuronal SH-SY5Y cells. OGDR-induced neuronal injury in SH-SY5Y cell lines is a classical *in vitro* cell model that mimics ischemia-reperfusion insult (Zhao et al. 2013). Ischemic injury results in the massive production

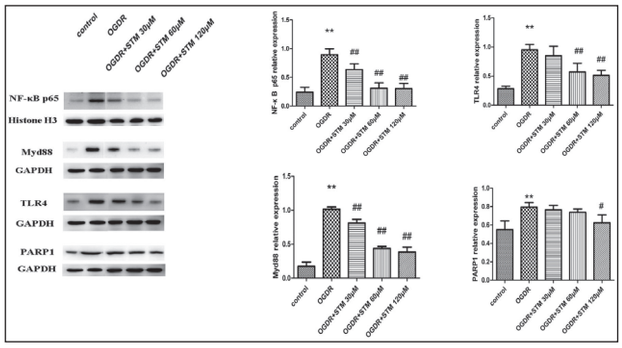

Fig. 4: STM inhibits the TLR4/PARP1/NF-κB signaling pathway. The expression of TLR4, Myd88, PARP1 and NF-κB P65 protein in the OGD/R group was notably increased compared with the control group ($p < 0.01$). In comparison, pretreatment with STM (30, 60 and 120μM) significantly inhibited Myd88 and NF-κB P65 protein expression as compared with the OGD/R group ($p < 0.01$). Pretreatment with STM (60 and 120μM) significantly reduced TLR4 protein expression as compared with the OGD/R group ($p < 0.01$). And pretreatment with STM (120μM) significantly repressed PARP1 expression as compared with the OGD/R group ($p < 0.01$). All data were obtained from at least three independent experiments. The results are represented as means ± S.D. * $p < 0.05$ versus control, ** $p < 0.01$ versus control; $^{\#}$ $p < 0.05$ versus OGDR, $^{\#\#}$ $p < 0.01$ versus OGDR by one- way ANOVA and LSD post hoc test.

of reactive oxygen species (ROS), which directly damages main cellular components. The restoration of oxygen levels in hypoxic tissues stimulates ROS production (Wang et al. 2016). And ROS could induce neuronal cell death in a time- and dose-dependent manner (Fukui 2016). In our study, STM significantly reduced the OGDR-induced ROS production, which implies that STM alleviated the OGDR-induced oxidative stress.

The protective activity of STM in the oxidative stress mediated disruption of mitochondrial membrane following OGDR-induced injury was evaluated. The mitochondrial membrane potential (ΔΨm) is generated by the special configuration of the outer and inner mitochondrial membranes. This ΔΨm decreases and membrane instability increases under conditions of mitochondrial dysfunction. Disruption of ΔΨm is one of the earliest events that occur following the onset of cellular apoptosis (Qi et al. 2010). Loss of mitochondrial membrane is mostly due to activation of mitochondrial permeability transition pore which leads to the release of Cytochrome C from mitochondria and then triggers apoptotic signals (Susin et al. 1998). OGDR resulted in mitochondrial depolarization, which in turn influences apoptotic process in SH-SY5Y cells (Weng et al. 2017). Our results showed that pretreatment with STM elevated the ΔΨm notably, suggesting the improvement of mitochondrial dysfunction in OGDR-induced SH-SY5Y cells.

NF-κB is a major transcriptional regulator of inflammation, which can be rapidly activated in the acute phase of cerebral ischemia (Chen et al. 2018), and the activation of the NF-κB pathway in neurons could promote the transcription of inflammatory genes (Nurmi et al. 2004). Furthermore, OGDR could induce the NF-κB signaling pathway activation in SH-SY5Y cells because the phosphorylation of IκBα and NF-kB p65 was observed 12 h following reoxygenation. NF-κB may be activated by multiple factors, of which TLR4 is one of the most important factors. Downregulation of the TLR4-dependent NF-κB signaling pathway could protect the brain against ischemic injury (Liu et al. 2017). In the present study, the TLR4/NF-κB signaling pathway was activated in SH-SY5Y cells by OGDR because the TLR4 expression and the nuclear translocation of NF-κB p65 were increased 24 hours following reoxygenation. The expression of TLR4, Myd88 and nuclear NF-κB p65 was reduced significantly in the STM treated groups, suggesting the attenuation of the activated TLR4/NF-κB signaling pathway. Repression of inflammation by STM after OGDR could be related to the downregulation of the expression of TLR4, Myd88 and inhibition of NF-κB nuclear translocation. TLR4 has two main signal transduction pathways (Myd88-dependent signaling pathway and Myd88- independent signaling pathway) that activate NF-κB in inflammation (Zhu et al. 2018). STM could downregulate the expression of TLR4 and Myd88 in this study, suggesting that STM modified NF-κB signaling via the Myd88-dependent signaling pathway.

The excessive ROS and mitochondrial dysfunction not only induces the apoptotic cascade, but also activates poly (ADP-ribose) polymerase (PARP). And PARP1 is a nuclear enzyme that can regulate the expression of various inflammatory genes (Pacher and Szabo 2008). After binding to damaged DNA, PARP1 accomplishes its activation and auto-poly (ADP-ribosylation) that is critical for DNA repair. However, excessive activation of PARP1 leads to intracellular depletion of β-nicotinamide adenine dinucleotide (NAD^+) and adenosine triphosphate (ATP), driving cells into energy depletion, mitochondrial dysfunction and cell death (Jagtap and Szabo 2005). On the other hand, PARP1 acts as a co-activator of the NF-κB to regulate the expression of a number of important inflammatory cytokines including inducible nitricoxide synthase (iNOS), monocyte chemotactic protein-1 (MCP-1), and adhesion molecules (Hassa and Hottiger 2002). For instance, lipopolysaccharides (LPS) could induce protein expression of PARP1 and TLR4 inhibition could reduce the upregulation of PARP1. PARP1 exerted a critical role by promoting phospho-NF-κB p65 nuclear translocation. PARP1 was a determining factor in TLR4-mediated inflammation in endothelial cells after LPS stimulation (Peng et al. 2012). Our results indicate that STM treatment could inhibited PARP1 in OGDR challenged SH-SY5Y cells.

In summary, our study showed that STM ameliorated OGDR-induced neuronal injury *in vitro* by attenuating increases in ROS levels and suppressing apoptosis, at least in part, via TLR4/PARP1/NF-κB pathway.

4. Experimental

4.1. Materials

Swertiamarin (S3927) was provided by Selleck Chemicals. Anti- TLR4, anti-Myd88, anti-NF-κB p65 and anti-PARP1 antibodies were purchased from Cell Signaling Technology (Beverly, MA, USA).

4.2. Cell culture

SH-SY5Y cells, a human-derived neuroblastoma cell line, were obtained from the ATCC (Manassas, VA, USA) and grown as monolayers in DMEM supplemented with 10 % heat-inactivated FBS. SH-SY5Y cells were incubated at 37 °C in a humidified atmosphere containing 5 % CO_2. To avoid changes in cell characteristics, caused by extended culture, all experiments were conducted with cells between passages 15 and 25. To maintain exponential growth, each cell culture was subcultured every 3 days using trypsin/ethylenediaminetetraacetic acid treatment. Before experiment, SH-SY5Y cells were pre-treated for 2 h with different concentrations of swertiamarin (30, 60, 120 μM).

4.3. Oxygen-glucose deprivation and reoxygenation (OGDR)

To establish an *in vitro* ischemic injury model, SH-SY5Y cells were first incubated in glucose- and serum-free DMEM in an anaerobic humidified chamber filled with 95 % N_2 and 5 % CO_2 for 4 h at 37 °C (mimic oxygen glucose deprivation). Afterwards, the SH-SY5Y cells were then cultured in a normal medium under normoxic conditions and re-oxygenated for 24 h. Normoxic control cells without OGDR were placed in norm-oxygenated complete medium.

4.4. Cell viability and cytotoxicity assays

The SH-SY5Y cells were cultured in 96-well plates at a density of 3×10^3 cells per well in DMEM medium for 24 h. Cells were incubated with different concentrations of STM for another 24 h. Cell viability was determined using a CCK-8 kit (Beyotime Biotechnology, China) according to the manufacturer's instructions. The absorbance was determined at 450 nm using a spectrophotometer (BioTek, Winooski, VT, USA).

4.5. Mitochondrial membrane potential assay

To determine the mitochondrial membrane potential, cells were stained with a JC-1 assay kit (Bioswamp) according to the manufacturer's instructions and subsequently analyzed by flow cytometry with the CXP software 2.0.

4.6. Measurement of intracellular ROS

To evaluate the levels of intracellular ROS, cells were treated with CM-H_2DCFDA for 1 h at 37 °C in an atmosphere of 5 % CO_2, then harvested, and washed three times with PBS. Fluorescence intensity was then measured by flow cytometry at an excitation wavelength of 488 nm and an emission wavelength of 525 nm. Data analyses were performed using the CXP software 2.0 (Beckman Coulter, Pasadena, CA, USA).

4.7. Neuronal apoptosis

The proportion of apoptotic cells was measured using an Annexin V-FITC/PI assay with an Annexin V-FITC/PI apoptosis detection kit (Beyotime Inst, China) in accordance with the manufacturer's instructions. Briefly, neuronal cells were cultured in 60 mm cell culture plates (1×10^6 cells/well), subjected to OGDR, harvested by trypsinization and washed three times with ice-cold PBS. The treated cells were then resuspended in 200 μL of binding buffer. After Annexin V-FITC (10μL) and PI (10μL) were added, the cells were incubated at 4 °C for 30 min. After that, 300 μL of Binging Buffer was added. Then flow cytometry was performed for the detection of apoptotic cells. Each experiment was repeated three times. Data analyses were performed using CXP software 2.0.

4.8. Western blot analysis

The whole cell lysate was prepared to evaluate the expression level of TLR4, Myd88 and PARP1. The nuclear extracts were obtained to evaluate the expression level of nucleus NF-κB p65 by using a nuclear/cytoplasmic isolation kit (Beyotime Institute of Biotechnology, Beijing, China). The protein concentration was determined using the bicinchoninic acid (BCA) assay and samples were stored at -80 °C. Equal amounts of protein were separated with 10 % sodium dodecyl sulfate (SDS)-polyacrylamide gel electrophoresis. After electrophoresis, the gels were transferred onto polyvinylidene difluoride (PVDF) membranes, which were blocked with Tris-buffered saline containing 5 % nonfat milk at 4 °C. Then, the membranes were incubated overnight at 4 °C in solution containing 0.1 % Tween 20, 5 % nonfat milk and the following primary antibodies: TLR4 (1:1000); Myd88 (1:1000); NF-κB p65 (1:2000); PARP1 (1:1000); GAPDH (1:1000); Histone H3 (1:1000). After three washes in Tris-buffered saline Tween 20, the membranes were incubated with HRP-conjugated secondary antibodies for 2 h at room temperature and subsequently processed for enhanced chemiluminescence (ECL) detection using potent ECL kit (MULTISCIENCES, China) and a chemiluminescence detection system (IS4000MM Pro, Kodak, USA). GAPDH or Histone H3 was used as an internal index.

4.9. Data analysis

Data were expressed as mean±S.D. The significant differences between groups were assessed with SPSS version 13.0. The differences between group means were calculated by one-way ANOVA with LSD post hoc analysis. Difference was considered statistically significant when $p < 0.05$, and extremely significant when $p < 0.01$.

Acknowledgments: This work is financially supported by Training Programme for Key Young and Middle-aged Medical Talents by Heath and Family Planning Commission of Wuhan Municipality (2018).

Conflicts of interest: The authors report no conflicts of interest.

References

Chen S, Yin W, Bi K, Lu B (2018) MicroRNA-497 attenuates cerebral infarction in patients via the TLR4 and CREB signaling pathways. Int J Mol Med 42: 547-556.

del Zoppo GJ (2010) Acute anti-inflammatory approaches to ischemic stroke. Ann N Y Acad Sci 1207: 143-8.

Fuentes B, Tejedor ED (2014) Stroke: The worldwide burden of stroke--a blurred photograph. Nat Rev Neurol 10: 127-8.

Fukui K (2016) Reactive oxygen species induce neurite degeneration before induction of cell death. J Clin Biochem Nutr 59: 155-159.

Hassa PO, Hottiger MO (2002) The functional role of poly(ADP-ribose)polymerase 1 as novel coactivator of NF-kappaB in inflammatory disorders.. Cell Mol Life Sci 59: 1534-53.

Jagtap P; Szabo C (2005) Poly(ADP-ribose) polymerase and the therapeutic effects of its inhibitors. Nat Rev Drug Discov 4: 421–440.

Kumar A, Negi G, Sharma SS (2011) JSH-23 targets nuclear factor-kappa B and reverses various deficits in experimental diabetic neuropathy: effect on neuroinflammation and antioxidant defence. Diabetes Obes Metab 13: 750-8.

Liu X, Zhang X, Wang F, Liang X, Zeng Z, Zhao J, Zheng H, Jiang X, Zhang Y (2017) Improvement in cerebral ischemia-reperfusion injury through the TLR4/NF-κB pathway after Kudiezi injection in rats. Life Sci 191: 132-140.

Macrez R, Ali C, Toutirais O, Le Mauff B, Defer G, Dirnagl U, Vivien D (2011) Stroke and the immune system:from pathophysiology to new therapeutic strategies. Lancet Neurol 10: 471–80.

Mahesh R, Jung HW, Han CH, Cho CW, Park YK (2011) Joongpoongtang 05 (JP05) confers neuroprotection via anti-apoptotic activities in Neuro-2a cells during oxygen-glucose deprivation and reperfusion. Toxicol In Vitro 25: 177-84.

Molina CA, Alvarez-Sabín J (2009) Recanalization and reperfusion therapies for acute ischemic stroke. Cerebrovasc Dis 27: S162–S167.

Nurmi A, Lindsberg PJ, Koistinaho M, Zhang W, Juettler E, Karjalainen-Lindsberg ML, Weih F, Frank N, Schwaninger M, Koistinaho J (2004) Nuclear factor-kappaB contributes to infarction after permanent focal ischemia. Stroke 35: 987-991.

Pacher P, Szabo C (2008) Role of the Peroxynitrite-Poly(ADP-Ribose) Polymerase Pathway in Human Disease. Am J Pathol 173: 2-13.

Park SY, Chae SY, Park JO, Lee KJ, Park G (2017) Kalopanacis Cortex extract-capped gold nanoparticles activate NRF2 signaling and ameliorate damage in human neuronal SH-SY5Y cells exposed to oxygen-glucose deprivation and reoxygenation. Int J Nanomedicine 12: 4563-4578.

Peng X, Li W, Zhang W (2012) Poly(ADP-ribose) polymerase 1 inhibition protects human aortic endothelial cells against LPS-induced inflammation response. Acta Biochim Biophys Sin (Shanghai) 44: 911-7.

Qi F, Li A, Zhao L, Xu H, Inagaki Y, Wang D, Cui X, Gao B, Kokudo N, Nakata M, Tang W (2010) Cinobufacini, an aqueous extract from Bufo bufo gargarizans Cantor, induces apoptosis through a mitochondria-mediated pathway in human hepatocellular carcinoma cells. J Ethnopharmacol 128: 654-61.

Régnier CH, Song HY, Gao X, Goeddel DV, Cao Z, Rothe M (1997) Identification and characterization of an IkappaB kinase. Cell 90: 373-83.

Sun LP, Xu X, Hwang HH, Wang X, Su KY, Chen YL (2016) Dichloromethane extracts of propolis protect cell from oxygen-glucose deprivation induced oxidative stress via reducing apoptosis. Food Nutr Res 60: 30081.

Susin SA, Zamzami N, Kroemer G (1998) Mitochondria as regulators of apoptosis: doubt no more. Biochim Biophys Acta 1366: 151-65.

Ulbrich F, Kaufmann K, Roesslein M, Wellner F, Auwärter V, Kempf J, Loop T, Buerkle H, Goebel U (2015) Argon mediates anti-apoptotic signaling and neuroprotection via inhibition of toll-like receptor 2 and 4. PLoS One 10: e0143887.

Wang J, Han D, Sun M, Feng J (2016) Cerebral ischemic postconditioning induces autophagy inhibition and a HMGB1 secretion attenuation feedback loop to protect against ischemia reperfusion injury in an oxygen glucose deprivation cellular model. Mol Med Rep 14: 4162–4172.

Weng Y, Lin J, Liu H, Wu H, Yan Z, Zhao J (2017) AMPK activation by Tanshinone IIA protects neuronal cells from oxygen-glucose deprivation. Oncotarget 9: 4511-4521.

Wu T, Li J, Li Y, Song H (2017) Antioxidant and hepatoprotective effect of swertiamarin on carbon tetrachloride-induced hepatotoxicity via the Nrf2/HO-1 pathway. Cell Physiol Biochem 41: 2242-2254.

Wu T, Zhang Q, Song H (2018) Swertiamarin attenuates carbon tetrachloride (CCl4)-induced liver injury and inflammation in rats by regulating the TLR4 signaling pathway. Braz J Pharm Sci 54: e17449.

Xu XY, Cheng QL, Li HL, Su HL (2010) Protective effect of swertiamarin on H2O2-induced apoptosis of mice cardiomyocytes. Medicinal Plant 1: 47-49.

Yu CZ, Li C, Pei DS, Zong YY, Shi Q, Wen XR, Guan QH, Hang D, Hou XY, Zhang GY (2009) Neuroprotection against transient focal cerebralischemia and oxygen-glucose deprivation by interference with GluR6-PSD95 protein interaction. Neurochem Res 34: 2008–2021.

Zhang Q, Chen K, Wu T, Song H (2019) Swertiamarin ameliorates carbon tetrachloride-induced hepatic apoptosis via blocking the PI3K/Akt pathway in rats. Korean J Physiol Pharmacol 23: 21-28.

Zhang T, Wang H, Li Q, Huang J, Sun X (2014) Modulating autophagy affects neuroamyloidogenesis in an in vitro ischemic stroke model. Neuroscience 263: 130-137.

Zhao LP, Ji C, Lu PH, Li C, Xu B, Gao H (2013) Oxygen glucose deprivation (OGD)/re-oxygenation-induced in vitro neuronal cell death involves mitochondrial cyclophilin-D/P53 signaling axis. Neurochem Res 38: 705-713.

Zhu S, Tang S, Su F (2018) Dioscin inhibits ischemic stroke-induced inflammation through inhibition of the TLR4/MyD88/NF-κB signaling pathway in a rat model. Mol Med Rep 17: 660-666.